Chemical Science

EDGE ARTICLE

View Article Online
View Journal | View Issue

Cite this: *Chem. Sci.*, 2018, **9**, 623

A durable monolithic polymer foam for efficient solar steam generation†

Qiaomei Chen,[a] Zhiqiang Pei,[b] Yanshuang Xu,[a] Zhen Li,[a] Yang Yang,[a] Yen Wei*[a] and Yan Ji*[a]

Received 6th July 2017
Accepted 1st November 2017

DOI: 10.1039/c7sc02967e

rsc.li/chemical-science

Efficient and cost-effective solar steam generation requires self-floating evaporators which can convert light into heat, prevent unnecessary heat loss and greatly accelerate evaporation without solar concentrators. Currently, the most efficient evaporators (efficiency of ~80% under 1 sun) are invariably built from inorganic materials, which are difficult to mold into monolithic sheets. Here, we present a new polymer which can be easily solution processed into a self-floating monolithic foam. The single-component foam can be used as an evaporator with an efficiency at 1 sun comparable to that of the best graphene-based evaporators. Even at 0.5 sun, the efficiency can reach 80%. Moreover, the foam is mechanically strong, thermally stable to 300 °C and chemically resistant to organic solvents.

Introduction

Solar steam generation holds great promise for a broad range of important industrial processes including power generation, seawater desalination and wastewater treatment. As natural sunlight is too weak, solar steam generation usually requires pricey optical concentrators. Meanwhile, photo-thermal materials which can convert sunlight into heat are introduced to facilitate evaporation. Nevertheless, bulk water heating still has low efficiency because much heat is consumed to heat bulk water or is lost to the atmosphere.[1,2] Recently, it has been recognized that confining the photo-thermal material generated heat at the air–water interface using a self-floating evaporator is an effective solution to this problem. Substantial progress has been made in the past 3 years by building efficient evaporators with plasmonic absorbers and carbon materials.[3–16] For example, using airlaid paper as the substrate for assembled gold nanoparticles, an efficiency of 77.8% at 6 sun illumination was obtained.[9] Besides gold nanoparticles, aluminum nanoparticles made it possible to reach an efficiency of 91% at 6.0 sun.[13] Research on solar steam generation without optical concentration is also exciting. Chen's group demonstrated a floating solar receiver capable of generating 100 °C steam under ambient air conditions at 1 sun, despite having a low efficiency of 23%.[11] Most recently, Hu's group developed a novel carbon nanotube (CNT)-modified flexible wood (F-Wood/CNTs) for solar steam generation with an evaporation efficiency of 65% at 1 sun.[17] At 1 sun, the highest efficiency has reached 80–83% with evaporators made of graphene oxide (vapor temperature $T_{vap} = 41$ °C, evaporation efficiency $\eta = 82\%$,[4] $T_{vap} = 39$ °C and $\eta = 80\%$ (ref. 5)), carbon nanotubes ($T_{vap} = 32$ °C and $\eta = 82\%$),[6] graphene ($T_{vap} = 44$ °C and $\eta = 83\%$),[7] or nitrogen doped graphene ($T_{vap} = 100$ °C and $\eta = 80\%$).[8] Inorganic materials face a critical challenge in the fabrication of floating evaporators. Inorganic materials are normally powders rather than films. To be an efficient floating evaporator, assisting materials have to be used either as porous supports to allow water to fill in or insulating layers to prevent heat transferring to the bulk.[6,7,12,18] More often than not a multi-layer structure is used, which not only increases the fabrication complexity, but also sacrifices the durability. So far, there is only one case in which a single component was used (costly nitrogen-doped graphene foam[8]) to make a floating evaporator. As is well known, large areas of graphene foam are hard to process and scale up. When talking about square kilometers of water surface in the field, none of the present available evaporators are practically and economically viable. Moreover, there are other problems for different inorganic materials. For example, popular gold nanoparticles are expensive, easy to fuse, and susceptible to photo-bleaching.[19,20] Alumina-based materials need structural modification, cannot stand corrosive environments and are unsuitable for desalination for long service times.[13] Compared to inorganic materials (especially nano-materials) used for the evaporators, polymer foams have many innate advantages as they are inexpensive, suitable for monolithic large-scale fabrication, and intrinsically thermally insulating. Moreover, there are various mature methods to make and adjust porous structures.[21–24] However, making a highly efficient solar heat evaporator out of a single polymer is certainly not a low-hanging fruit. A good

[a]*MOE Key Laboratory of Bioorganic Phosphorus Chemistry & Chemical Biology, Department of Chemistry, Tsinghua University, Beijing 100084, China. E-mail: jiyan@mail.tsinghua.edu.cn; weiyen@tsinghua.edu.cn*

[b]*Simpson Querrey Institute for BioNanotechnology, Northwestern University, Chicago, Illinois 60611, USA*

† Electronic supplementary information (ESI) available. See DOI: 10.1039/c7sc02967e

interfacial photo-thermal evaporator should simultaneously fulfill the following requirements: (a) be able to effectively absorb and convert natural sunlight into heat without mirrors or lenses, (b) have the ability to float at the air–water interface, (c) have a low thermal conductivity to prevent heat loss to the bulk water, (d) have open porosity for water to go through, and (e) display excellent stability under various water conditions. It is challenging to integrate all of the above features in one single-component material. So far, few polymers have displayed broad light absorption within the whole solar spectrum range and have high photo-thermal conversion abilities. Besides, common polymers are susceptible to acids, bases and organic solvents. In fact, rare evaporators are made of polymers as photo-thermal agents. A solar-thermal evaporator with floating polymeric foams was put forward in a patent filed in 1966,[25] where carbon particles must be uniformly dispersed into polymers. However, polymer foams only act as the carrier for photothermal carbon materials. It was not an evaporator made of only one material. Polypyrrole (PPy) has been used for interfacial solar heating.[10] In this case, it has to be coated on stainless steel to get a porous structure. Although the hydrophobicity of the evaporator is self-healable, the efficiency is low (~60%). As PPy is used as a coating, delamination is a potential problem. Moreover, PPy is soluble in organic solutions. It remains very challenging to make an evaporator from any single-component materials including polymers.

Here, we designed and synthesized a new polymer for solar-driven water evaporation. Its foam, with the polymer as the only component, can be used as an evaporator. The foam is easy to prepare and scale up from low-cost raw chemicals. The foam evaporator can obtain a high evaporation efficiency at a low illumination intensity. At 1 sun, its efficiency is above 80% with excellent durability and stability, which makes it among one of the best evaporators. Moreover, even at 0.5 sun its efficiency can also reach 80%, which has never been reported in the past. According to our work, there is a large discrepancy between the widely used evaporation efficiency calculation and the heat loss. It should be noticed that this is a common problem in the field of solar evaporation. Despite it being a polymer foam, the evaporator has excellent solvent resistance, with little volume changes in various organic polar and non-polar solvents such as ethanol, acetone, chloroform, methylbenzene, tetrahydrofuran and *N*,*N*-dimethylformamide. When used for solar desalination, the salinities decrease to below 1 ppm, which is lower than the values obtained *via* distillation-based desalination.

Results and discussion

Preparation and characterization of the evaporator

To be an evaporator, first of all, the polymer should be able to absorb a wide range of solar light and effectively convert light into heat. We chose oligoaniline to build such a polymer. Oligoanilines share many common features with polyaniline such as excellent electro-activity and chemical redox activity. But in contrast to polyaniline, oligoanilines have well-defined molecular structures, good solubility in common solvents and flexibility for modification. We previously found that oligoanilines could convert infrared light into heat.[26] Further experiments with the same material showed that it could also respond to sunlight. For better photo-thermal conversion, a higher oligoaniline content in the polymer is preferred. Throughout the literature, we found that the condensation polymerization created by García *et al.*[27] and published in the journal Science two years ago is most desirable. In this reaction, diamine and paraformaldehyde can form a densely cross-linked network consisting mainly of the diamine derivate. Therefore, when we use an oligoaniline with amine ends (Fig. 1a), we can get a type of poly(1,3,5-hexahydro-1,3,5-triazine) (PHT) consisting of mainly aniline trimer. The structure of the polymer was confirmed by Fourier-transform infrared spectroscopy (FTIR), X-ray photoelectron spectroscopy (XPS) and elemental analysis (the details can be obtained from the ESI†). Another reason that we chose this reaction is because Hedrick *et al.*[27] have reported that such a type of highly cross-linked polymer possesses a high modulus, and excellent stability in organic solvents and solutions with pH > 3. As a solar evaporator stability must be considered seriously, so we checked the stability of this polymer. As shown in Fig. S3,† the evaporators undergo little volume changes after being soaked in methylbenzene (PhMe), ethanol (EtOH), tetrahydrofuran (THF), *N*,*N*-dimethylformamide (DMF), pH = 4 H_2SO_4 aqueous solution and pH = 12 NaOH aqueous solution for 24 h. The reason we chose these organic solvents is that they can represent organic solvents with different polarities, indicating that the polymer foam can resist almost all of the organic solvents. As with the potential applications, the polymer foam may be used to remove water from organic solvents with high boiling points, to purify the organic solvents, or to separate organic solvents with very different boiling points. The foam is thermally stable with a decomposition temperature of 300 °C (Fig. S8†). To verify the photo-thermal effect of such an oligoaniline containing PHT, we measured the temperature of it at 0.5 sun, 1 sun and 2 sun illumination. As shown in the IR thermal images (Fig. S10†), the temperatures of the evaporator rise to 47 °C, 67 °C and 101 °C, respectively, within just 10 s, revealing the excellent photo-thermal effect of the evaporator.

To enable self-floating on the water surface and allow free water transportation from the bulk to the surface, the polymer should be processed into a foam. There are various techniques to prepare polymer foams. Here, we chose a NaCl particulate leaching method (details can be obtained from the ESI†). Using this method, macroporous materials can be obtained. Previously reported highly efficient evaporators have normally had microporous structures, which have a great probability of being blocked in the field. The macroporous structure used here will greatly decrease clogging in real practice. The pore sizes can be flexibly tailored by the size of the NaCl particles. Moreover, the method is simple, low-cost, and easy to scale up. Furthermore, NaCl can be recycled. Utilizing the NaCl template, we just need to cast the solution into it and cure *in situ*. Here, to get a high evaporation efficiency and excellent mechanical strength, we chose NaCl particles with a size of less than 50 μm. After washing off the NaCl template with water, a foam was obtained. Fig. 1b presents the typical scanning electron microscopy (SEM)

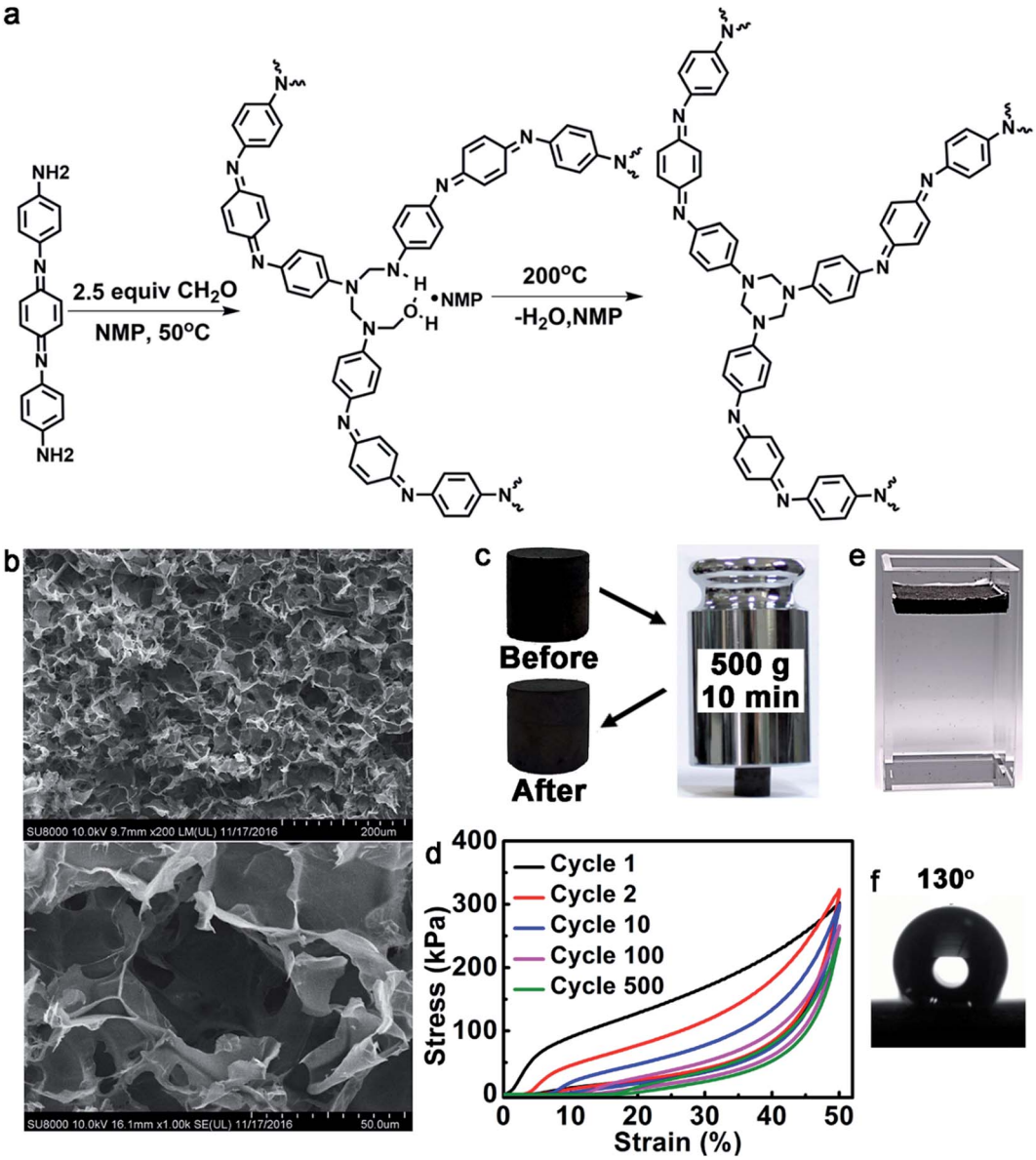

Fig. 1 Synthesis and characterization of the evaporator. (a) Synthesis of the polymer. (b) SEM images of the foam evaporator under low and high magnification. (c) Photographs of a cylindrical evaporator ($d = 10$ mm and $h = 10$ mm) supporting a weight of 500 g (the weight of the cylinder is about 25 mg). (d) Compressive stress–strain curves of the foam. (e) An optical image of the foam evaporator self-floating at the air–water interface. (f) The water-wetting performance of the foam evaporator.

images of the foam. The foam possesses excellent mechanical strength. As shown in Fig. 1c, it can support a weight of 500 g (about 2000 times heavier than itself, generating a pressure of about 62.4 kPa). The polymer foam can maintain its elasticity for at least 500 loading/unloading cycles with a compressive strain of 50% (Fig. 1d), although the maximum stress decreased from 302 to 246 kPa and the height was also shortened by about 15%. The compressive modulus of the first cycle was calculated to be 2.67 MPa, which is about 95 times that of the reported graphene aerogel.[28]

As shown in Fig. 1e, the evaporator can float well at the air–water interface. The density of the evaporator was calculated to be about 32.2 mg cm^{-3} *via* precise weight and volume measurements. Another reason that we chose oligoaniline was that it is hydrophobic without doping (after doping with acid it is hydrophilic).[29] Such hydrophobicity will help the material to float on the water surface. As shown in Fig. 1f, the water contact angle of the bulk evaporator reaches 130° without any surface modification, which is normally necessary to get a surface with such high hydrophobicity.[30–33] Moreover, in contrast to hydrophobic coatings, such a bulk hydrophobicity property will not be damaged during its service life. Since our polymer foam is macroporous, after swelling in water for about 10 min, water can ultimately go through the interconnecting paths of the foam from the bottom to the surface. All of the efficiency experiments were started after the foam had been wetted with

water. Moreover, the hydrophobicity may endow the foam with some advantages over the hydrophilic ones such as more robust floating due to superior water repellency and anti-contamination.[10,34,35]

The optical properties were studied using a UV-vis/NIR spectrometer equipped with an integrating sphere at ambient temperature ranging from 250 to 2250 nm. As shown in Fig. 2a, the porous polymer photo-thermal evaporator demonstrates a relatively low total reflectance (less than 5% in the UV-vis region and no more than 16% in the whole measurement region). The transmission was nearly nonexistent. Assuming the absorption $A = 1 - T - R$, absorption was obtained, weighting 95.2% of the whole solar spectrum. The photo-thermal conversion is still very effective when the foam is floating on the surface of water. The IR thermal image shows that the temperature of the evaporator floating at the air–water interface rises to 46 °C at 1 sun within 15 min (Fig. 2b).

Evaporation efficiency

To some extent, the polymer foam can reduce the heat loss to bulk water. The dry polymer foam itself has a thermal conductivity as low as 0.057 W m^{-1} K^{-1}, which is much lower than those of most of the reported inorganic solar absorbers used for solar steam generation (*e.g.* nitrogen-doped graphene has a thermal conductivity of 9.0 ± 1.2 W m^{-1} K^{-1}, which is one of the lowest values among carbon-based materials).[8] As the foam has macroscopic channels instead of microscale ones, water will leak out quickly once it is taken out of the water. We cannot measure its thermal conductivity in the wet state, but the value is bound to be lower than that of pure water, leading to a reduction of heat lost to the bulk water. Moreover, the effect of the foam in blocking the heat loss to the water body is evident. As shown in Fig. 2c, the corresponding temperatures of the steam are much higher than those of water at about 4 cm below the surface. For example, the temperatures of the steam and water are 46.7 °C and 30.6 °C after 1 h illumination at 1 sun, respectively. And the higher the light intensity, the higher the related temperatures of the evaporator.

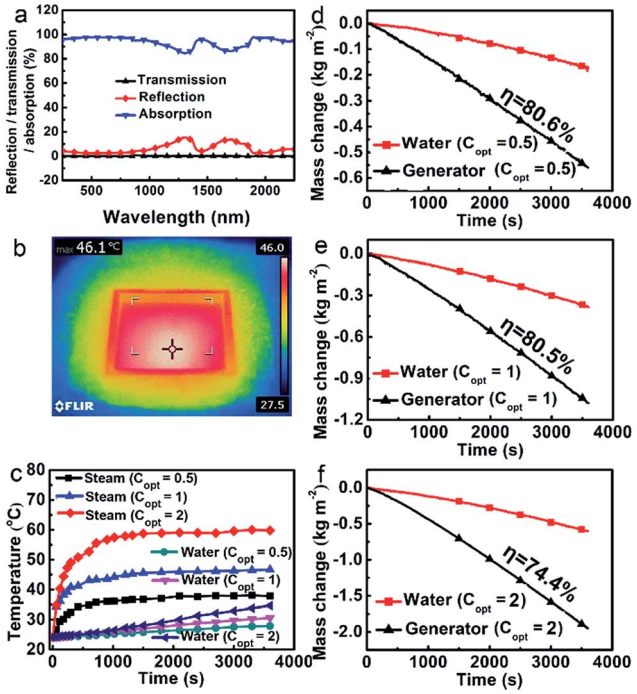

Fig. 2 The heat localization and solar steam generation performance of the evaporator. (a) The optical properties of the evaporator ranging from 250 to 2250 nm. (b) The surface temperature of the evaporator floating at the air–water interface after 15 min of solar illumination at $C_{opt} = 1$. (c) The corresponding temperatures of the steam and water at about 4 cm below the surface (all experiments were conducted in an ambient temperature of 24–25 °C with a humidity of 10–11%). (d–f) The mass changes over time with and without the evaporator under different optical concentrations C_{opt} of 0.5 (d), 1 (e) and 2 (f) (the dark evaporation rate is subtracted from all of the evaporation rate measurements).

The polymer evaporator enables a high evaporation efficiency at a low solar light intensity. Water can be constantly pumped to the hot region, and the evaporation rate reaches equilibrium after the initial transient period (about 15 min). As shown in Fig. 2d–f, it is evident that the evaporation rates of water using the evaporator are much higher than those of water without the evaporator under all optical concentrations (C_{opt}). For instance, the evaporation rate using the evaporator under $C_{opt} = 1$ (which is 1 sun) is about 1.1687 kg m^{-2} h^{-1}, 2.7 times that of the water without the evaporator (0.4346 kg m^{-2} h^{-1}). As the evaporation rates vary with the environment, generally, the evaporation efficiency η was used to evaluate the efficiency of the evaporators.[3–15] Calculated from those data (see ESI†), the evaporation efficiency η reaches as high as 80.5% under a solar intensity of 1 kW m^{-2} (1 sun). This puts it among the highest efficiency evaporators at normal sunlight illumination.[4–8] Even at 0.5 sun, the efficiency is still about 80.6%.

It should be noted that there is a large discrepancy between the efficiencies calculated by (100% − calculated heat loss) (~59.5–68.5%) and the efficiency (~80.5% at 1 sun) calculated by the evaporation rate according to the formula commonly used in this field ($\eta = \dot{m}h_{LV}/C_{opt}P_0$) (detailed calculations of the heat loss and the efficiency derived from the evaporation rate are shown in the ESI†). When we checked the literature and calculated the available data, we found that this large discrepancy was a common phenomenon (please see some examples of detailed calculations in ESI†). On one hand, this discrepancy may come from the errors of the empirical formulas or coefficients used to calculate the heat losses and experimental errors. On the other hand, it should be pointed out that the commonly used formula to calculate the evaporation efficiency depends on the evaporation rate, which can be greatly affected by experimental conditions such as humidity, the room temperature and steam diffusion rate. When comparing the efficiency of different systems, it is better to check the heat loss at the same time.

Durability and stability of the evaporator

Durability and stability are important aspects for solar steam generation. Fig. 3a shows that the evaporation mass changes are

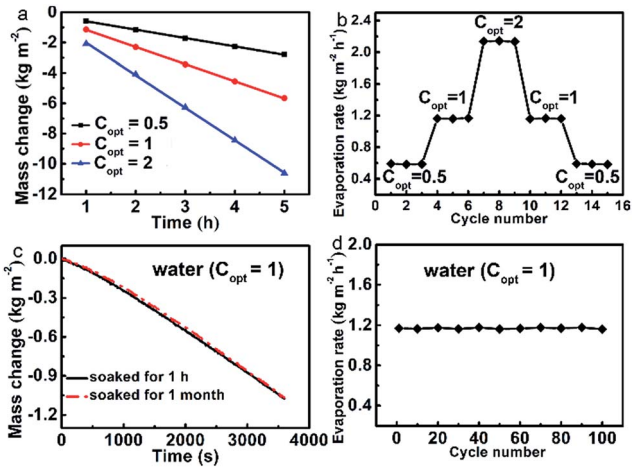

Fig. 3 Durability and stability of the evaporator. (a) The evaporation mass changes of water under different C_{opt} within 5 hours. (b) The evaporation cycle performance of the evaporator under different solar concentrations. (c) Evaporation rate curves of the evaporator soaked in water after 1 h and 1 month. (d) The evaporation cycle performance of the evaporator in water over 100 cycles, with each cycle sustained for 1 h.

linearly maintained under all C_{opt} with illuminations as long as 5 h. The evaporation rates under a series of C_{opt} were measured *via* cycle experiments, of which each C_{opt} was repeated three times and each cycle sustained for 1 h (Fig. 3b). It reveals that the evaporator has excellent stability and durability under different C_{opt}. Moreover, after being soaked in water for one month, the evaporation rate is still as high as 1.1608 kg m^{-2} h^{-1} (Fig. 3c), the corresponding evaporation efficiency of which is 80.0%. We further conducted the cycle evaporation experiments 100 times in water at $C_{opt} = 1$. As shown in Fig. 3d, the evaporation rates are nearly maintained constant. After being dried, the evaporator still has a water contact angle of about 129° (Fig. S12†), which further justifies its stability and durability.

Relevant water treatments of the evaporator

The solar-driven water evaporation of the evaporator can be used for various relevant water treatments. We investigated the desalination efficiency at first. As shown in Fig. 4a, the concentrations of all of the metal ions in 3.5 wt% NaCl solution and 1 wt% mixed solution are decreased to below 1 ppm.

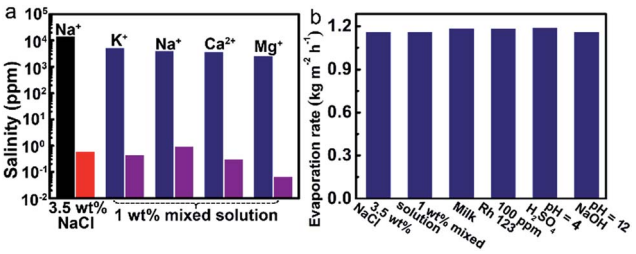

Fig. 4 Environmentally-relevant water treatments. (a) The measured concentrations of metal ions before and after desalination. (b) The corresponding water evaporation rates of different water solutions.

Secondly, the water evaporation rates ($C_{opt} = 1$) of different types of water solution ranging from 1.1598 to 1.1902 kg m^{-2} h^{-1}, which are close to that of pure water (Fig. 4b). The calculated evaporation efficiencies are within the range of 79.9% to 82.0%. Rh 123 is completely removed in the condensed water vapor (the details can be seen in the ESI, Fig. S13†). Moreover, after solar light-driven water evaporation of the acidic and basic solutions, the pHs of the collected condensed water vapors all approach 7. All of the above results demonstrate the versatility of the evaporator in various conditions of water treatments.

Conclusions

Solar energy is renewable, abundant and freely available to us. Harvesting solar light and converting it into heat is not only useful for water evaporation. As an effective photo-thermal material, the polymer presented here can also be used for other areas such as sensing, imaging, thermophotovoltaics, solvent purification, phase changing and light/thermal detectors, to name a few. To be fair, there is a big issue with the material that we synthesized here, that is, that paraformaldehyde is used during the synthesis. Even though melamine, which also uses formaldehyde as a starting material, has been used for dining plates, spoons and other tableware, the material reported here which is very similar to melamine needs further thorough investigation when it is used for drinking water purification. Moreover, whether this material can stand one year's exposure to sunlight needs to be tested. However, the work here paves a first step for using polymer foam alone as an efficient evaporator, which may offer many advantages that could not be matched by the inorganic photo-thermal materials currently used. For example, in the foam used here, the density could be easily modulated by the concentration of the casting solution; the sizes of the pores could also be flexibly controlled by the size of the NaCl particles used to meet various practical applications; and the polymer can also be processed into film or other configurations. With better optimizations and more effort in this area, it is very likely that evaporators made of polymer foams will surpass the performance of the material presented here and that of inorganic materials. Meanwhile, the cost will drop. In that case, cost effective and easy-to-implement polymer films can be used as solar evaporators in many more countries and states with water shortages.

Conflicts of interest

There are no conflicts to declare.

Acknowledgements

This research was supported by the National Science Foundation of China (no. 20161300524 and 21274075). We thank Prof. Jia Zhu and Dr Lin Zhou of Nanjing University for their help with the efficiency calculations. We also thank Dr Xiaowen Yu of Tsinghua University for the XPS analysis. We are grateful to the referees for their many detailed and significant suggestions,

which not only led to essential improvements of our paper but will also contribute to our following works.

Notes and references

1 O. Neumann, A. S. Urban, J. Day, S. Lal, P. Nordlander and N. J. Halas, *ACS Nano*, 2012, **7**, 42–49.
2 O. Neumann, C. Feronti, A. D. Neumann, A. Dong, K. Schell, B. Lu, E. Kim, M. Quinn, S. Thompson and N. Grady, *Proc. Natl. Acad. Sci. U. S. A.*, 2013, **110**, 11677–11681.
3 H. Ghasemi, G. Ni, A. M. Marconnet, J. Loomis, S. Yerci, N. Miljkovic and G. Chen, *Nat. Commun.*, 2014, **5**, 4449.
4 X. Hu, W. Xu, L. Zhou, Y. Tan, Y. Wang, S. Zhu and J. Zhu, *Adv. Mater.*, 2016, **29**, 1604031.
5 X. Li, W. Xu, M. Tang, L. Zhou, B. Zhu, S. Zhu and J. Zhu, *Proc. Natl. Acad. Sci. U. S. A.*, 2016, **113**, 13953–13958.
6 Y. Wang, L. Zhang and P. Wang, *ACS Sustainable Chem. Eng.*, 2016, **4**, 1223–1230.
7 L. Shi, Y. Wang, L. Zhang and P. Wang, *J. Mater. Chem. A*, 2017, **5**, 16212.
8 Y. Ito, Y. Tanabe, J. Han, T. Fujita, K. Tanigaki and M. Chen, *Adv. Mater.*, 2015, **27**, 4302–4307.
9 Y. Liu, S. Yu, R. Feng, A. Bernard, Y. Liu, Y. Zhang, H. Duan, W. Shang, P. Tao and C. Song, *Adv. Mater.*, 2015, **27**, 2768–2774.
10 L. Zhang, B. Tang, J. Wu, R. Li and P. Wang, *Adv. Mater.*, 2015, **27**, 4889–4894.
11 G. Ni, G. Li, S. V. Boriskina, H. Li, W. Yang, T. Zhang and G. Chen, *Nat. Energy*, 2016, **1**, 16126.
12 L. Zhou, Y. Tan, D. Ji, B. Zhu, P. Zhang, J. Xu, Q. Gan, Z. Yu and J. Zhu, *Sci. Adv.*, 2016, **2**, e1501227.
13 L. Zhou, Y. Tan, J. Wang, W. Xu, Y. Yuan, W. Cai, S. Zhu and J. Zhu, *Nat. Photonics*, 2016, **10**, 393–398.
14 G. Wang, Y. Fu, X. Ma, W. Pi, D. Liu and X. Wang, *Carbon*, 2017, **114**, 117–124.
15 Q. Jiang, L. Tian, K. K. Liu, S. Tadepalli, R. Raliya, P. Biswas, R. R. Naik and S. Singamaneni, *Adv. Mater.*, 2016, **28**, 9400–9407.
16 A. Politano, P. Argurio, G. Di Profio, V. Sanna, A. Cupolillo, S. Chakraborty, H. A. Arafat and E. Curcio, *Adv. Mater.*, 2017, **29**, 1603504.
17 C. Chen, Y. Li, J. Song, Z. Yang, Y. Kuang, E. Hitz, C. Jia, A. Gong, F. Jiang and J. Zhu, *Adv. Mater.*, 2017, **29**, 1701756.
18 M. Ye, J. Jia, Z. Wu, C. Qian, R. Chen, P. G. O'Brien, W. Sun, Y. Dong and G. A. Ozin, *Adv. Energy Mater.*, 2016, 1601811.
19 E. Ju, Z. Li, M. Li, K. Dong, J. Ren and X. Qu, *Chem. Commun.*, 2013, **49**, 9048–9050.
20 L. Li, K. Liang, Z. Hua, M. Zou, K. Chen and W. Wang, *Polym. Chem.*, 2015, **6**, 2290–2296.
21 M. Carta, R. Malpass-Evans, M. Croad, Y. Rogan, J. C. Jansen, P. Bernardo, F. Bazzarelli and N. B. McKeown, *Science*, 2013, **339**, 303–307.
22 P. J. Waller, F. Gándara and O. M. Yaghi, *Acc. Chem. Res.*, 2015, **48**, 3053–3063.
23 R. Huang, X. Zhu, H. Tu and A. Wan, *Mater. Lett.*, 2014, **136**, 126–129.
24 M. K. Joshi, H. R. Pant, A. P. Tiwari, C. H. Park and C. S. Kim, *Chem. Eng. J.*, 2015, **275**, 79–88.
25 J. F. Hardy, Andover, M. E. Jordan, Walpole and A. I. Medalia, *U.S. Pat.*, 3,282,327, 1966.
26 Q. Chen, X. Yu, Z. Pei, Y. Yang, Y. Wei and Y. Ji, *Chem. Sci.*, 2017, **8**, 724–733.
27 J. M. García, G. O. Jones, K. Virwani, B. D. McCloskey, D. J. Boday, G. M. ter Huurne, H. W. Horn, D. J. Coady, A. M. Bintaleb and A. M. S. Alabdulrahman, *Science*, 2014, **344**, 732–735.
28 Y. Li, J. Chen, L. Huang, C. Li, J. D. Hong and G. Shi, *Adv. Mater.*, 2014, **26**, 4789–4793.
29 Q. Qian, J. Wang, F. Yan and Y. Wang, *Angew. Chem. Int. Ed.*, 2014, **53**, 4465–4468.
30 C. R. Crick, J. A. Gibbins and I. P. Parkin, *J. Mater. Chem. A*, 2013, **1**, 5943–5948.
31 V. H. Pham and J. H. Dickerson, *ACS Appl. Mater. Interfaces*, 2014, **6**, 14181–14188.
32 L. Liu, C. Chen, S. Yang, H. Xie, M. Gong and X. Xu, *Phys. Chem. Chem. Phys.*, 2016, **18**, 1317–1325.
33 J. Gu, P. Xiao, J. Chen, F. Liu, Y. Huang, G. Li, J. Zhang and T. Chen, *J. Mater. Chem. A*, 2014, **2**, 15268–15272.
34 Y. Liu, J. Chen, D. Guo, M. Cao and L. Jiang, *ACS Appl. Mater. Interfaces*, 2015, **7**, 13645–13652.
35 J. Ge, H. Y. Zhao, H. W. Zhu, J. Huang, L. A. Shi and S. H. Yu, *Adv. Mater.*, 2016, **28**, 10459–10490.